Moisture effects on microbial protein biosynthesis from ammonium and nitrate in an unfertilised grassland

Michaela K. Reay [a,*], Nadine Loick [b], Richard P. Evershed [a,e], Christoph Müller [c,d,e], Laura Cardenas [b,e]

[a] *Organic Geochemistry Unit, School of Chemistry, University of Bristol, Cantock's Close, Bristol, BS8 1TS, UK*
[b] *Rothamsted Research, North Wyke, Okehampton, Devon, EX20 2SB, UK*
[c] *Institute of Plant Ecology, Justus Liebig University Giessen, 35392, Giessen, Germany*
[d] *School of Biology and Environmental Science and Earth Institute, University College Dublin, Belfied, Dublin 4, Ireland*
[e] *Liebig Centre for Agroecology and Climate Impact Research, Justus Liebig University, Germany*

ABSTRACT

Incorporation of nitrogen (N) into soil microbial protein is central to the soil N cycle to mitigate N losses and support plant N supply. However, the effect of factors, such as water filled pore space (WFPS), which influence inorganic N transformations and losses, and thus microbial incorporation, are only poorly understood. This work aimed to bridge this gap, using compound-specific ^{15}N-stable isotope probing to quantify microbial assimilation into the largest defined soil organic N pool, protein-N. This approach applied differentially ^{15}N-labelled ammonium nitrate (NH_4NO_3) to an unfertilised UK grassland in a soil mesocosm study over 10 days. The soil microbial community showed a strong preference for NH_4^+ over NO_3^-, which varied with WFPS (85% > 55% > 70%). This preference decreased for amino acids further in biosynthetic proximity to the transamination step in amino acid biosynthesis. Combined incorporation of NH_4^+ and NO_3^- increased total hydrolysable amino acid-N concentration linked to WFPS (55% ~ 85% > 70%). Incorporation rates of applied ^{15}N showed the same trend as NH_4^+ preference with WFPS (85% > 55% > 70%), which is related to microbial activity and nutrient mobility. Despite differences in incorporation, when normalised to soil available N, incorporation was comparable in the short-term. Mechanistic control of WFPS via assimilation into the largest soil organic N pool is important to mitigate potential positive feedbacks to N losses and support N supply to plants.

1. Introduction

Organic nitrogen (N) concentration in soil is much higher than inorganic N (Schulten and Schnitzer, 1998). Due to its size (Friedel and Scheller, 2002), rapid assimilation (Knowles et al., 2010) and turnover rate (Jones and Kielland, 2012; Wanek et al., 2010), the active portion of the organic pool is central to the soil N cycle, and fate of N. However, the direct effect of soil properties, such as moisture content, on soil organic nitrogen (N_{org}) biosynthesis is not fully understood (Thomsen et al., 1999). The hydrological regime of soil influences the microbial community structure (Banerjee et al., 2016) and thus the biochemical soil properties (Giacometti et al., 2013). Changes in soil moisture dynamics are expected under climate change due to changing rainfall patterns and evapotranspiration (Berg and Sheffield, 2018). This will affect N losses via gaseous emissions (e.g., the climate relevant trace gas nitrous oxide,

N_2O and other reactive N gases) and leaching.

Soil moisture content influences nutrient mobility and availability to the microbial community and affects microbially mediated N transformations (Misra and Tyler, 1999). Water filled pore space (WFPS) is well-correlated with aerobic and anaerobic microbial activity, and associated processes of respiration, mineralisation and denitrification (Harrison-Kirk et al., 2013). Moisture is also a controlling factor for seasonal changes in microbial biomass (Wardle, 1998). However, the relationship between N transformations and water content is not simple. For example, the source of N_2O is controlled by WFPS, with heterotrophic nitrification and nitrification dominating at lower WFPS, while denitrification increases with WFPS, due to increasingly anaerobic conditions, alongside increased nutrient mobility (Davidson, 1993; Linn and Doran, 1984; Luo et al., 1999; Saggar et al., 2013). Using the *Ntrace* tool it has been shown that, besides changing the sources of N_2O,

---

increasing WFPS decreased other gross N transformation rates associated with NH_4^+ and NO_3^- (Loick et al., 2021). Assimilation of inorganic N into the larger N_{org} pool will affect N availability for the above-mentioned processes, and thus is central to mechanistically underpin N_2O fluxes and potential mitigation strategies (Müller et al., 2014; Zhang et al., 2015).

However, it is still relatively unknown how N_{org} and microbial assimilation of inorganic N are influenced by soil moisture at a molecular level. This is despite microbial N assimilation being of key importance in retention of nutrients in soil and microbial growth efficiency (Herron et al., 2009; Six et al., 2006), and immobilisation as N_{org} will feedback on nutrient availability for other N cycling processes. Increases in microbial biomass N and a lower microbial C:N ratio were observed at higher water holding capacities, indicating effects on microbial growth (Xue et al., 2017). Previous studies have found an effect of soil moisture on microbial immobilisation, with a marked decrease in ^{15}N immobilisation, using chloroform fumigation extraction, in dry soils (5% *w/w*), despite little effect on ^{13}C immobilisation (Herron et al., 2009).

To date, quantification of immobilisation into the microbial N pool, and potential effects of moisture, has been achieved indirectly via numerical ^{15}N tracing (Loick et al., 2021), or using bulk approaches, e.g., chloroform-fumigation-extraction (Herron et al., 2009). Probing the biomolecular fate of N into newly biosynthesized microbial N_{org} can offer a direct way of quantifying microbial biosynthesis and elucidate relationships with soil moisture. Compound-specific ^{15}N-stable isotope probing (SIP) targets newly biosynthesized microbial protein, via the constituent amino acids (AAs). This approach directly determines the assimilation of the applied ^{15}N labelled substrates, e.g., fertilisers, into the largest defined N_{org} pool in the soil, both in free (FAAs) and bound (BAAs) forms (Friedel and Scheller, 2002; Schulten and Schnitzer, 1998). It has been applied to quantify the incorporation of inorganic N (Charteris et al., 2016; Reay et al., 2023), organic N (Knowles et al., 2010; Reay et al., 2022) and N_2 (Chiewattanakul et al., 2022) into newly biosynthesized soil microbial protein.

Previous applications of compound-specific ^{15}N-SIP have confirmed direct assimilation of organic nitrogen compounds, and differences in processing of inorganic N forms. Based on these findings, the fundamental approach can now be applied to clarify the functional relationships between microbial protein biosynthesis and influencing factors such as the water content. This will provide insight into the fate of N at a biomolecular level and how this may affect other N cycling processes. The aim of this study is to elucidate the impact of soil moisture (i) on AA biosynthesis in a UK grassland soil and (ii) on the N partitioning of differing inorganic N forms into the soil microbial protein pool. To achieve this, ammonium nitrate (NH_4NO_3) was applied as either $^{15}NH_4NO_3$ or $NH_4^{15}NO_3$ to a grassland soil mesocosm at varying WFPS (55%, 70% and 85%) (Loick et al., 2021). Assimilation into the AA pool was determined via compound-specific ^{15}N-SIP, alongside determination of soil NO_3^- and NH_4^+ concentrations and ^{15}N enrichment. It was hypothesised that (i) assimilation of ammonium (NH_4^+) would be higher than nitrate (NO_3^-), and (ii) assimilation of applied N would increase with increasing WFPS.

2. Methods

2.1. Experimental set-up

The soil preparation, experimental design and analysis for inorganic N pools were previously published in Loick et al. (2021). Briefly, soil, to a depth of 15 cm was collected in May 2015 from Rothamsted Research, North Wyke, Devon, UK (50°46′10″N, 3°54′05″W). The grassland area had not received fertilisation or inputs from grazing for over 20 years. The soil is classified as a clayey pelostagnogley soil of the Hallsworth series (44% clay, 40% silt, 15% sand (*w/w*); (Clayden and Hollis, 1984)). Initial soil properties can be found in Table S1. After collection, soil was air dried (30% gravimetric water content) from 50% (58% WFPS),

sieved (2 mm) and stored at 4 °C until the experiment. Cores (4.5 cm diameter, 7.5 cm depth) were prepared to a bulk density of 0.8 g cm^{-3}, reflecting field conditions. The soil moisture was adjusted to 55%, 70% or 85% WFPS and incubated at 20 °C. For each WFPS treatment, two ^{15}N labelling substrates were used: (i) $^{15}NH_4NO_3$ and (ii) $NH_4^{15}NO_3$, both applied at 50 atom% and at a rate equivalent to 75 kg N ha^{-1}. The cores were destructively sampled after $t = 0.2, 1, 2, 3, 4, 7$ and 10 d. At each time point, extractable NH_4^+, NO_3^- and NO_2^- were quantified, and ^{15}N enrichment determined, as outlined in Loick et al. (2021). Additionally, at each time step, a sub-sample was frozen (−20 °C), subsequently lyophilised and ground in preparation for AA analyses.

2.2. Amino acid preparation and analyses

Total hydrolysable AA (THAAs), representative of the soil protein pool (Roberts and Jones, 2008), were extracted using acid hydrolysis under an N_2 atmosphere (6 M HCl, 24 h, 100 °C). The hydrolysates were subsequently collected via centrifugation, dried and redissolved in 0.1 M HCl for cation exchange chromatography. The THAA fraction was isolated using Dowex®50WX8 in H$^+$ form and eluted with 2 M NH_4OH. The dried THAA fraction was derivatised to *N*-acetyl, *O*-isopropyl derivates (NAIP) in two stages. First, THAAs were propylated with isopropanol and acetyl chloride (4:1 *v/v*). After excess derivatising reagent was removed, THAAs were acetylated using triethylamine, acetic anhydride and acetone (2:1:5 *v/v/v*) (Corr et al., 2007). Norleucine (Nle; 100 μl of 400 μg ml^{-1} in 0.1 M HCl) was added as an internal standard for quantification.

Individual amino acid derivatives were quantified using GC (Agilent Technologies 7890B GC, Agilent Technologies, CA, USA). Data was acquired and analysed using Agilent OpenLab CDS Chemstation (Rev C.01.07[27]; Agilent Technologies). AAs were separated using a DB-35 capillary column (60 m × 0.32 mm i.d., 0.5 μm phase thickness) and He carrier gas at a constant flow of 2.0 ml min^{-1}. The temperature programme was 70 °C (2 min) to 150 °C at 15 °C min^{-1}, to 210 °C at 2 °C min^{-1} and a final temperature of 270 °C (8 °C min^{-1}; 10 min) (Chiewattanakul et al., 2022). An external standard of AAs was used to monitor instrument performance, identification and calculation of AA-specific response factors for quantification compared to the internal standard. The external standard comprised of 14 AAs (alanine (Ala), aspartic acid (Asp), glutamic acid (Glu), glycine (Gly), hydroxyproline (Hyp), leucine (Leu), lysine (Lys), norleucine (Nle), phenylalanine (Phe), proline (Pro), serine (Ser), threonine (Thr), tyrosine (Tyr) and valine (Val)) in 0.1 M HCl.

The ^{15}N enrichment of individual AAs as NAIP derivatives were determined using GC-C-IRMS. The IRMS (ThermoFinnigan Delta^{Plus} XP IRMS, Thermo Electron Corp., Waltham, MA, USA) was coupled with a ThermoFinnigan Trace 2000 GC via a ThermoFinnigan Combustion III Interface. The oxidation reactor was composed of copper and nickel wires maintained at 1030 °C. The ^{15}N enrichments of individual AAs were determined relative to that of a monitoring gas with known N isotopic composition and in-house standards. AA δ^{15}N values were accepted when standard values were with ± 1σ of the duplicate analyses of the sample AA NAIP derivatives. Data was acquired and analysed using IsoDat NT 3.0 (Thermo Electron Corp.). The GC column was the same as for GC analyses, with a carrier gas flow of 1.4 ml min^{-1}. The temperature programme was 40 °C (5 min hold), then heated to 120 °C (15 °C min^{-1}), to 180 °C (3 °C min^{-1}), to 210 °C (1.5 °C min^{-1}), and finally to 270 °C (5 °C min^{-1}; 1 min hold). All analyses were run in duplicate, and only accepted when the σ<5% of ^{15}N enrichment. Additionally, an in-house standard of AAs with known ^{15}N enrichments was analysed and values were only accepted when within ±1σ.

2.3. Data analysis

^{15}N enrichments of individual AAs are reported as atom fractions, and as percentage incorporated (%I) into each pool as derived from

applied ^{15}N as $^{15}NH_4NO_3$ or $NH_4^{15}NO_3$ at $t = 0$ following:

$$\%I = \frac{mol^E\left(^{15}N\right)_p}{mol^E\left(^{15}N\right)_g}100 \qquad \text{(Eq. 1)}$$

Where $mol(^{15}N)_g$ is the ^{15}N in applied ^{15}N-labelled fertiliser and $mol^E(^{15}N)_p$ is the total amount of ^{15}N in above ambient concentration in the individual AA pool. This is determined from the pool size (moles of ^{14}N and ^{15}N) and the atom fraction excess ($x^E(^{15}N)$):

$$x^E\left(^{15}N\right) = x\left(^{15}N\right)_p - x\left(^{15}N\right)_C \qquad \text{(Eq. 2)}$$

Where $x(^{15}N)_p$ is the atom fraction of ^{15}N in the pool at each sampling time point, and $x(^{15}N)_C$ is the atom fraction of ^{15}N in the pool without ^{15}N addition. Partitioning of soil retained ^{15}N into inorganic pools and THAAs were calculated in the same way using:

$$\%R = \frac{mol^E\left(^{15}N\right)_p}{mol^E\left(^{15}N\right)_R}100 \qquad \text{(Eq. 3)}$$

Where $mol(^{15}N)_R$ is the moles of ^{15}N in all determined soil pools (NH_4^+, NO_3^-, NO_2^- and THAAs). This was conducted on the combined $^{15}NH_4NO_3$ and $NH_4^{15}NO_3$ treatments, to account for influence of added N label, assuming only WFPS would have an effect on soil N partitioning, as ^{15}N was only added as a tracer.

Unless otherwise stated, all graphs and data analysis were carried out in R v4.1.2. (R Studio 2021). Significance levels were set at $p < 0.05$. Normality was checked visually using qqplot plots and heterogeneity using residual plots. Linear mixed-effects modelling was applied to evaluate the significance of the labelled N form ($^{15}NH_4^+$ or $^{15}NO_3^-$) and WFPS on amino acid incorporation. WFPS and labelled N form were fixed effects, while time and mesocosm were random effects. Where combined $^{15}NH_4NO_3$ and $NH_4^{15}NO_3$ treatments were used (amino acid concentrations, soil ^{15}N partitioning), WFPS was used as a fixed effect, and time and mesocosm were random effects. To determine the difference between rates of incorporation, separation of 95% confidence intervals for fitted linear regressions was evaluated. One-way ANOVAs and t-tests were used to determine differences in total incorporation at the end of the experimental period.

3. Results

3.1. Amino acid concentrations

The THAA-N concentration, as a proxy for protein-N, did not vary between the different ^{15}N labels for the same WFPS treatment ($F(1,108) = 0.677$, $p = 0.698$; Fig. S1). Therefore, the effect of WFPS on AA-N concentrations was tested on the combined results of both $^{15}NH_4NO_3$ and $NH_4^{15}NO_3$ applications (Fig. 1). Following the application of
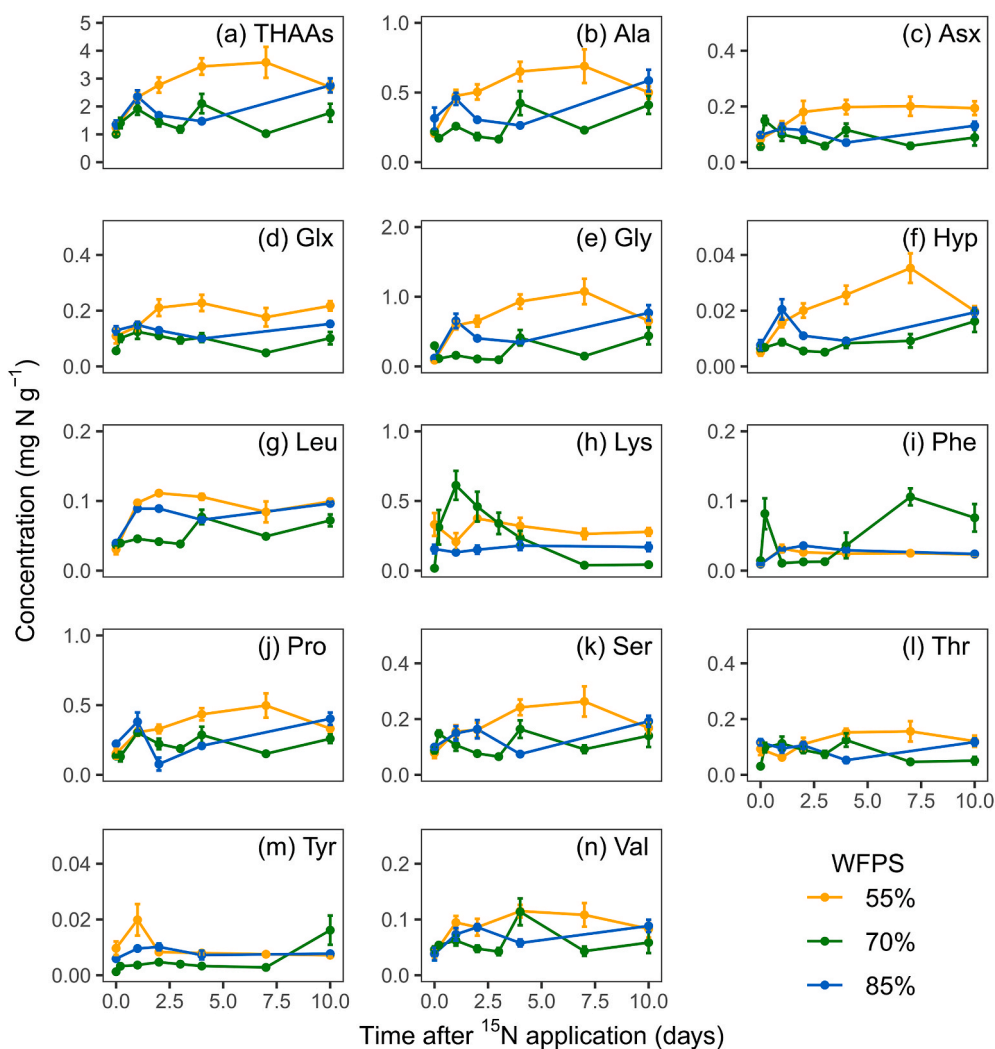
Fig. 1. Soil total hydrolysable amino acid (a) and individual hydrolysable amino acid (b–n) concentrations at differing WFPS. Values are mean for the $^{15}NH_4NO_3$ and $NH_4^{15}NO_3$ treatments $\pm$ SE ($n = 6$).

fertiliser, an increase in THAA-N concentrations was detected for all WFPS treatments. After 1 d, the effect on protein concentration diverged depending on WFPS, with a significant effect of WFPS on THAA-N concentration ($F_{(2, 95)} = 21.314$, $p < 0.001$). THAA-N concentrations increased at 55% WFPS, which was significantly higher than $t = 0$ at 10 d (t-test, $p = 0.044$). THAA-N concentration for the 85% WFPS treatment was also significantly higher at 10 d compared to $t = 0$ (t-test, $p < 0.001$), although decreased between 1 and 4 d. THAA-N concentrations in the 70% WFPS treatment showed similar levels to $t = 0$ ($p = 0.371$) at 10 d. Within individual AAs, the effect of WFPS was significant for all AAs (Table S2). Most AAs showed the same trend with different WFPS treatments as the THAA-N pool (e.g., Ala, Asx, Glx, Gly, Hyp, Pro, Ser, Thr). Two AAs, Lys and Phe (Fig. 1), showed slightly different patterns. Lys (Fig. 1h) showed an initial pronounced increase in concentrations at 70% WFPS, declining from day 2 onwards, while an initial decrease was detected at 55% WFPS. Phe (Fig. 1i) concentrations spiked initially, but stayed at levels similar to $t = 0$ from $t = 1$–3 d and increased after 4 d.

3.2. AA ^{15}N enrichment

The enrichment of individual AAs (as atom% ^{15}N) is presented in Fig. 2 following application of $^{15}NH_4NO_3$ or $NH_4^{15}NO_3$. For the $^{15}NH_4NO_3$ treatment, the ^{15}N enrichment increased linearly for all AAs, except for the secondary AA Hyp. Generally, enrichment was highest in the 85% WFPS treatment, and the 70% and 55% treatments had comparable ^{15}N enrichments, except at day 10, where enrichment of four AAs (Ser, Thr, Gly and Phe) was higher at 70% WFPS.

Changes in ^{15}N enrichment following application of $NH_4^{15}NO_3$ were more variable, with enrichment initially increasing from $t = 0$–1 d, plateauing then a later increase in ^{15}N enrichment after day 4. Looking at differences between WFPS treatments following $NH_4^{15}NO_3$ application, the majority of AAs exhibited the highest ^{15}N enrichment at 70% WFPS, while the 85% and 55% treatments were comparable. The ^{15}N enrichment of AAs after $NH_4^{15}NO_3$ application was lower for most AAs than after $^{15}NH_4NO_3$ amendment. The exception were Hyp and Thr, which gave the opposite result, with higher enrichment for $NH_4^{15}NO_3$, and Pro and Ser, where ^{15}N enrichment after 10 days were comparable between the two ^{15}N forms.

3.3. Incorporation into the THAA pool

Individual ^{15}N enrichments of AAs were used to calculate the incorporation of the applied ^{15}N, to account for the different pool sizes and determine if there were differences in assimilation into soil microbial protein. The analysis of the ^{15}N incorporation into soil microbial protein revealed differences in incorporation of NH_4^+-N and NO_3^--N and total fertiliser-N within, and between WFPS treatments.

3.3.1. Differential assimilation of $^{15}NH_4^+$ and $^{15}NO_3^-$

The differentially labelled application of NH_4NO_3 showed differences in the assimilation of $^{15}NH_4^+$ and $^{15}NO_3^-$ within WFPS treatments. At 55% WFPS, the rate of assimilation over 10 days for $^{15}NH_4^+$ was 0.184% d^{-1} ($r^2 = 0.794$) and for $^{15}NO_3^-$ was 0.145% d^{-1} ($r^2 = 0.411$). However, the maximum incorporation observed at 10 d was significantly higher for $^{15}NH_4^+$ than $^{15}NO_3^-$ (t-test, $p < 0.001$). Similarly, the rate of assimilation did not vary for the two ^{15}N labels for the 70% WFPS treatment, and incorporation after 10 days was comparable (t-test, $p = 0.34$). The assimilation rate at 85% WFPS was higher for $^{15}NH_4^+$ (0.255% day^{-1}; $r^2 = 0.951$) than for $^{15}NO_3^-$ (0.096% day^{-1}; $r^2 = 0.720$), as confirmed by a 95% CI. Finally, incorporation after 10 d was
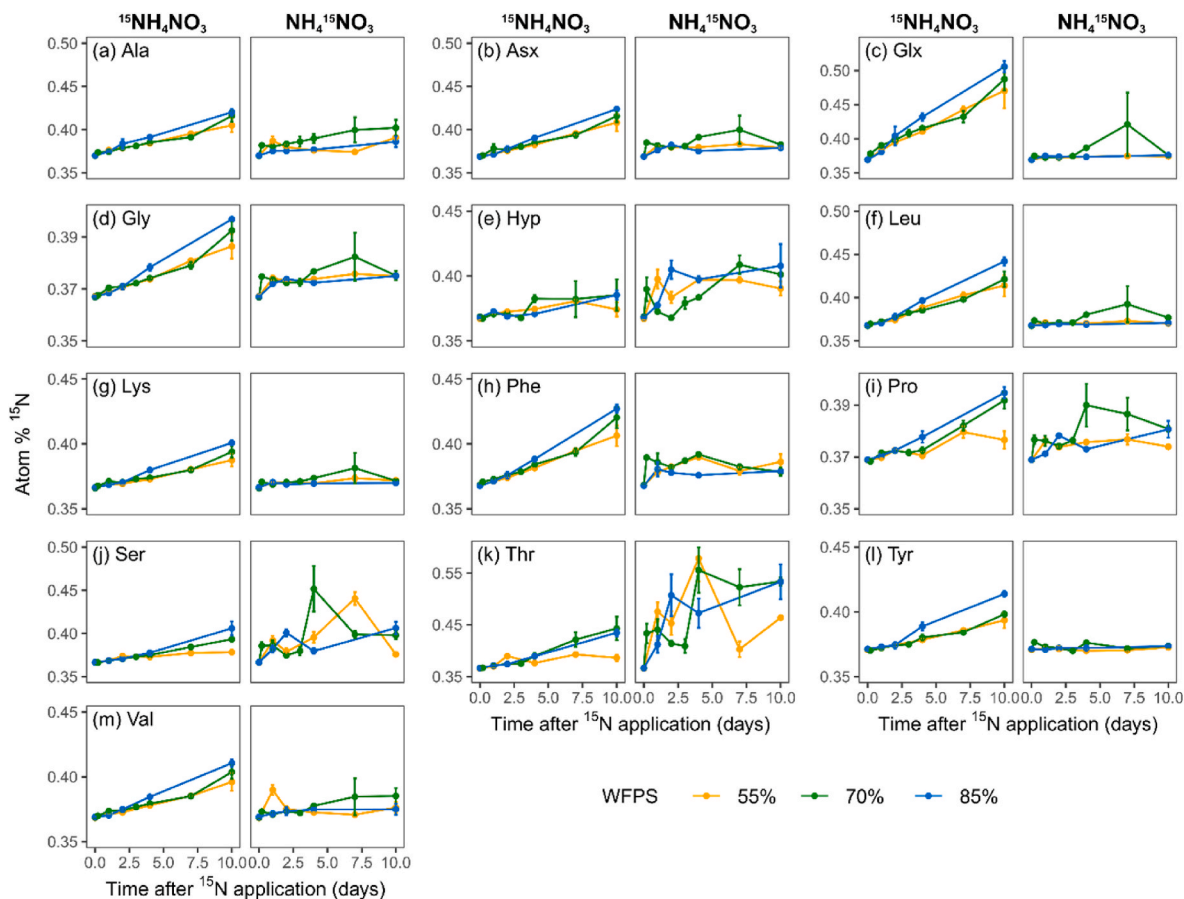
Fig. 2. ^{15}N enrichment of individual soil amino acids over 10 days after application of $^{15}NH_4NO_3$ or $NH_4^{15}NO_3$ to soil mesocosms at differing WFPS. Values are mean ($n = 3$) $\pm$ SE.

significantly higher for $^{15}NH_4^+$ (t-test, $p < 0.001$).

3.3.2. Effect of WFPS on $^{15}NH_4^+$ and $^{15}NO_3^-$ assimilation

Different WFPS treatments indicated soil moisture altered assimilation of the applied ^{15}N labels. For NH_4NO_3 labelling, there was no difference in incorporation rates between WFPS treatments (Fig. 3b), as confirmed by the 95% CI, and incorporation after 10 d was not significantly different between WFPS treatments (One-way ANOVA; $p = 0.058$). However, there were differences in rates of incorporation following $^{15}NH_4NO_3$ application (Fig. 3a), with 70% WFPS was significantly lower than the 55% and 85% WFPS treatments (Table S3). For all WFPS treatments, it was relatively consistent that the rates of assimilation of ^{15}N into individual AAs were higher for $^{15}NH_4NO_3$ compared to $NH_4^{15}NO_3$ (Table S3; Fig. 4), although some AAs displayed different trends. Hyp had a higher incorporation after 10 d for $^{15}NO_3^-$ and higher rates of incorporation at 70% and 85% for $^{15}NO_3^-$ (Fig. 4e) Similarly, Ser (Fig. 4j) exhibited higher $^{15}NO_3^-$ incorporation at 10 d for 55% and 70%, alongside higher rates of $^{15}NO_3^-$ incorporation, while there was no difference for 85% WFPS. Thr (Fig. 4k) also had comparable rates of NO_3^- and NH_4^+ incorporation for 55% and 70%, however, incorporation of NO_3^- was higher than NH_4^+ for the 85% WFPS treatment, alongside higher incorporation at 10 d (Tables S3 and S4).

3.3.3. Total consumption of ^{15}N-fertiliser

It was assumed that the combined assimilation of ^{15}N in the $^{15}NH_4NO_3$ and $NH_4^{15}NO_3$ treatments represented the total consumption of fertiliser. The sum of incorporation for the two treatments was also used to determine total assimilation of fertiliser N (Fig. 3c). Overall, there was a significant effect of WFPS alone on incorporation of fertiliser ^{15}N (F(2,64) = 16.918, $p < 0.001$), although a different N label alone did not significantly alter incorporation (F(1,64) = 0.217, $p = 0.643$). For the combined assimilation of fertiliser N, rates were 85% > 55%–70% (Table S3), and the incorporation after 10 d significantly varied (one-way ANOVA, $p = 0.044$), with 85% > 55%>70%. The 70% WFPS incorporation after 10 d was significantly lower than the 55% treatment (post-hoc Bonferroni, $p = 0.045$; Table S4). The individual AAs showed similar patterns of incorporation as the THAA pool, with variation for Thr, Ser, Hyp, as observed in the separated ^{15}N labelled treatments.

3.4. Effect of WFPS on partitioning of soil retained ^{15}N

To assess the effect of WFPS on partitioning of soil retained ^{15}N, the $^{15}NH_4NO_3$ and $NH_4^{15}NO_3$ treatments were combined, assuming the assimilation of $^{14}NH_4^+ = ^{15}NH_4^+$, and $^{14}NO_3^- = ^{15}NO_3^-$. The average ^{15}N accounted in soil pools after 10 d was $42 \pm 1.9\%$ of the total ^{15}N applied, and it is suggested that the unaccounted ^{15}N was contained in non-extractable inorganic pools, gaseous losses or other N_{org} pools that were beyond the scope of this study. To account for variability between treatments (27–52%) and elucidate the effect of WFPS on soil available N partitioning, the total ^{15}N retained in soil pools was used to indicate relative partitioning. Soil inorganic N concentrations and ^{15}N enrichments from Loick et al. (2021) were used to calculate %R (Eq. (3)) for inorganic N pools. The highest retention was found in the NH_4^+ and NO_3^- pools, as expected with the addition of $^{15}NH_4NO_3$ or $NH_4^{15}NO_3$. Yet, there were different trends in retention in these pools, which were influenced by the WFPS. Firstly, retention in the NH_4^+ pool was below 50% within both 0.2 d (70% WFPS only) and 1 d (all WFPS), while NO_3^- was above 50%. This is likely an artefact of adsorption of NH_4^+, meaning lower recovery by extraction. Subsequently, ^{15}N retained in the NH_4^+ pool decreased, with the largest decreases for 70% and 85% WFPS (Fig. 5a), with a significant effect of WFPS (F(2,32) = 19.446, $p < 0.001$). The opposite trends were observed for NO_3^- (Fig. 5b), where retention was highest for 70% and 85% WFPS compared to 55% WFPS, with a significant effect of WFPS (F(2,32) = 16.678, $p < 0.001$). Retention in the NO_2^- pool was low for all treatments relative to other determined soil pools (Fig. 5c), although WFPS significantly influenced partitioning into this pool (85% > 55% > 70%; F(2,32) = 75.995, $p < 0.001$). Partitioning into the THAA pool (Fig. 5d) was initially comparable between WFPS treatments (to 2 d), yet later diverged, with slower partitioning into 85% compared to 55%, and fluctuation in relative partitioning, as in inorganic N pools for 70% WFPS. WFPS significantly influenced partitioning into this pool across the 10-d period (F(2,32) = 7.583, $p = 0.002$), although there was little difference in partitioning at the end of the experiment ($p > 0.05$).

4. Discussion

The use of differentially ^{15}N-labelled NH_4NO_3 allowed the separation of the dynamics of these two key inorganic N inputs. This is the first time the two inorganic N forms have been added at the same time and traced directly into the microbial protein pool via compound-specific ^{15}N-SIP. This tested the microbial preference for an inorganic N form and not the effects of availability. The preferred assimilation of NH_4^+ over NO_3^- was observed for all WFPS treatments for incorporation into the THAA pool, although the effect varied depending on WFPS. This preference of NH_4^+ > NO_3^- for assimilation into THAAs has previously been observed in
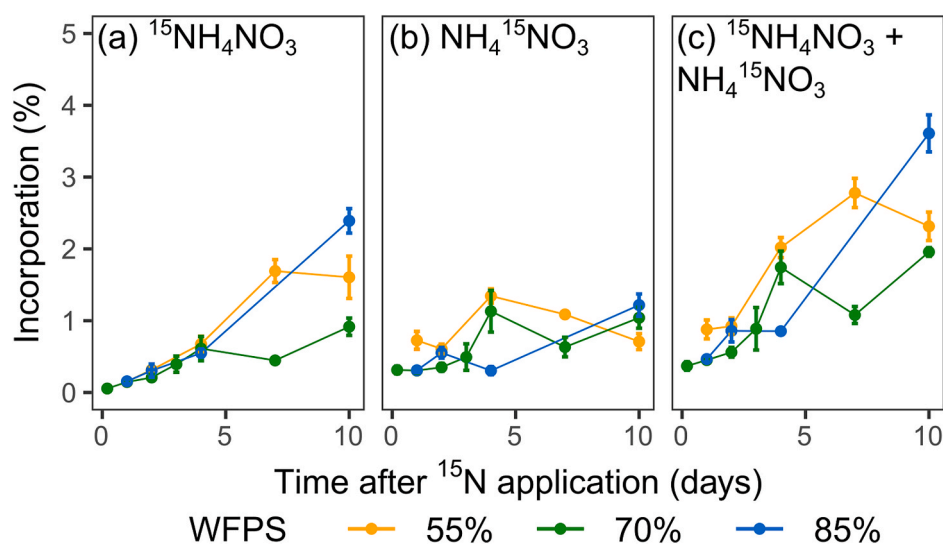
Fig. 3. Incorporation into the total hydrolysable amino acid pool following addition of (a) $^{15}NH_4NO_3$, (b) $NH_4^{15}NO_3$, and (c) total combined incorporation over 10 days at differing WFPS. Values are mean ($n = 3$) $\pm$ SE for (a) and (b) and $n = 6$ for (c).
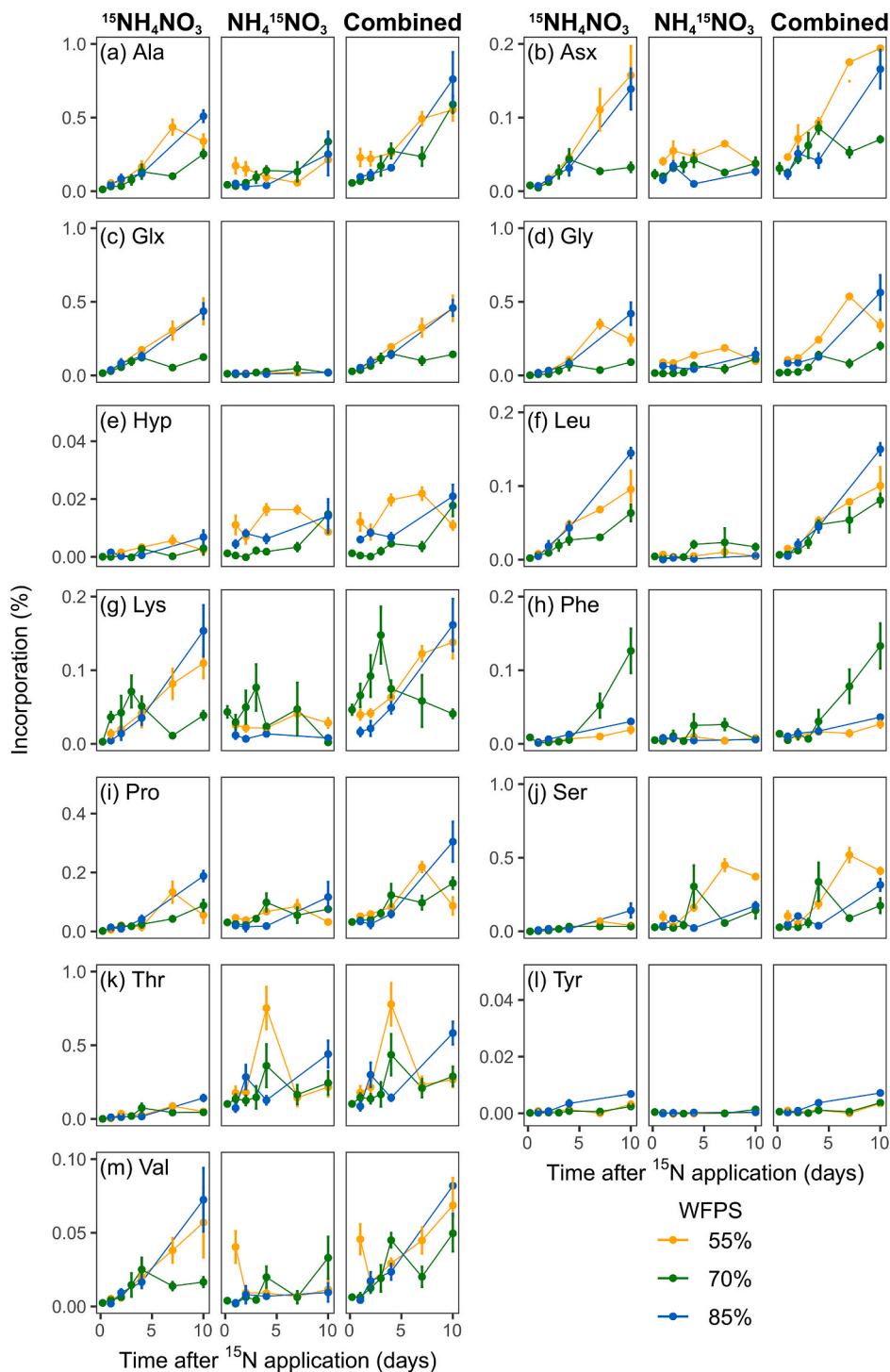
Fig. 4. Incorporation into the individual hydrolysable amino acid pool following addition of $^{15}NH_4NO_3$, $NH_4^{15}NO_3$, and total combined incorporation over 10 days at differing WFPS. Values are mean ($n = 3$) $\pm$ SE.

fertilised grasslands when applied separately (Charteris et al., 2016). Similar lower microbial nitrate utilisation has been observed via bulk measurements. For example, in a temperate grassland, microbial $^{15}NH_4^+$ uptake exceeded that of $^{15}NO_3^-$, determined via chloroform-fumigation-extraction, with temporal variations in preference which may be linked to climatic or soil property (e.g., moisture) variations (Liu et al., 2016). Further, where carbon has been applied alongside NH_4^+ and NO_3^-, this preference for NH_4^+ is retained (Christie and Wasson, 2001; Ma et al., 2020). This preference was attributed to the higher energy requirements for NO_3^- uptake and assimilation (via

reduction to NH_4^+) (Geisseler et al., 2010; Geisseler and Horwath, 2014; Recous et al., 1990; Rice and Tiedje, 1989). Observing this when NH_4NO_3 has been added together confirmed that this is a microbial preference rather than an artefact of N addition.

The $NH_4^+ > NO_3^-$ preference was observed for all treatments; however, the degree of preference did vary. At 85% WFPS, utilisation of NH_4^+ relative to NO_3^- was highest, and this was consistent with the largest decrease in NH_4^+ concentration (Loick et al., 2021), and ^{15}N retained in this pool (Fig. 5a). It is suggested that the higher moisture content aided nutrient mobility and thus availability to soil microbes (Misra and Tyler,
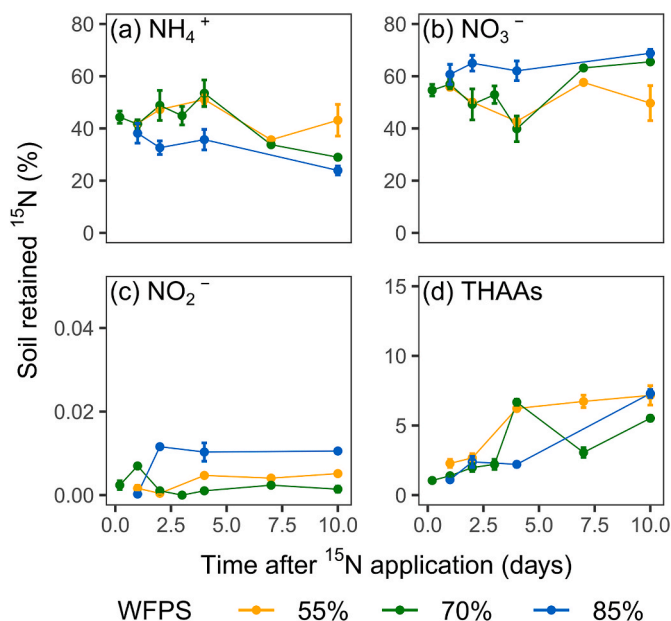
Fig. 5. Partitioning of soil-retained ^{15}N into (a) NH_4^+, (b) NO_3^-, (c) NO_2^- and (d) THAAs, from combined application of $^{15}NH_4NO_3$ and $NH_4^{15}NO_3$. Values are mean $\pm$ SE ($n = 3$). Note varying scales for clarity.

1999). This is supported by low adsorption rates of NH_4^+ at 85% WFPS (Loick et al., 2021). Furthermore, increased denitrification was observed compared to soils at lower WFPS, indicating an alternative fate of NO_3^- (Barrat et al., 2021; Butterbach-Bahl et al., 2013; Loick et al., 2021; Saggar et al., 2013). It was surprising that the preference for NH_4^+ was higher at 55% WFPS than at 70% WFPS, given hypothesised increases in nutrient mobility, and thus availability at higher WFPS. This suggested that there are several mechanisms influencing the uptake and assimilation of inorganic N. At 55% WFPS, there was a minimal decrease in extracted NH_4^+ (Loick et al., 2021), and potential rapid recycling of utilised $^{15}NH_4^+$ back into the NH_4^+ pool (e.g., via DNRA (dissimilatory

nitrate reduction to ammonia)). The lowest degree of preference for NH_4^+ *vs.* NO_3^- was observed at 70% WFPS, which also had the lowest NH_4^+ concentrations, alongside comparable rates of NH_4^+ adsorption to 55% WFPS. With lower NH_4^+ availability, it is assumed that NO_3^- is used as an alternative N source, despite higher energy costs. This grassland had relatively high OM content (11.7%), hence it is suggested there was sufficient C available to support NO_3^- assimilation as required at lower NH_4^+ concentrations, although a preference for NH_4^+ was still observed. The degree of preference observed for THAA biosynthesis (85% > 55%> 70%) also reflected CO_2 fluxes from a separate experiment conducted with the same conditions under a He/O_2 atmosphere (Cárdenas et al., 2003; Loick et al., 2021). This was conducted in parallel to the results presented herein over 13 d, with the same N loading, temperature and soil conditions, and gas sampled every 4 h. The observed CO_2 provides an indication of microbial activity and suggests higher microbial activity coincided with increased preference for NH_4^+, while decreased microbial respiration at 70% WFPS was linked to decreased assimilation of the applied ^{15}N label.

Within the THAA pool, the majority of individual AAs followed the same degree of preference for NH_4^+ over NO_3^- (85% > 55% > 70%). However, three AAs – Hyp, Ser and Thr – had differing trends and exhibited little difference between $^{15}NH_4^+$ and $^{15}NO_3^-$ treatments, or a preference for $^{15}NO_3^-$. Thr and Hyp are both further in biosynthetic proximity to the point where NH_2 is transferred to a C skeleton via glutamate dehydrogenase or glutamine synthetase (Reitzer, 2004), illustrated in Fig. 6. Thr is biosynthesized from Asx (Dong et al., 2012; Reitzer, 2014), however, this does not involve transamination, with NH_2 present in Asx from transamination to oxaloacetate, directly incorporated into Thr. Similarly, Hyp is biosynthesized from bound Pro, by prolyl-4-hydroxylase (Adams and Frank, 2003; Kanehisa et al., 2022) with no transamination step. There is also no transamination step for Pro biosynthesis from glutamate, proceeding via ɣ-glutamic semialdehyde following carboxyl reduction, which cycles to L-Δ^1-pyrroline-5-carboxylate, and a second reduction step yields Pro (Csonka and Leisinger, 2007). Pro did exhibit higher NH_4^+ assimilation over NO_3^-, however, this was only significant at 85% WFPS. Since the C: N ratio is conserved in the biosynthesis of Pro from Glu, this biosynthetic proximity likely reflects the observed preference for Glx in Pro, although
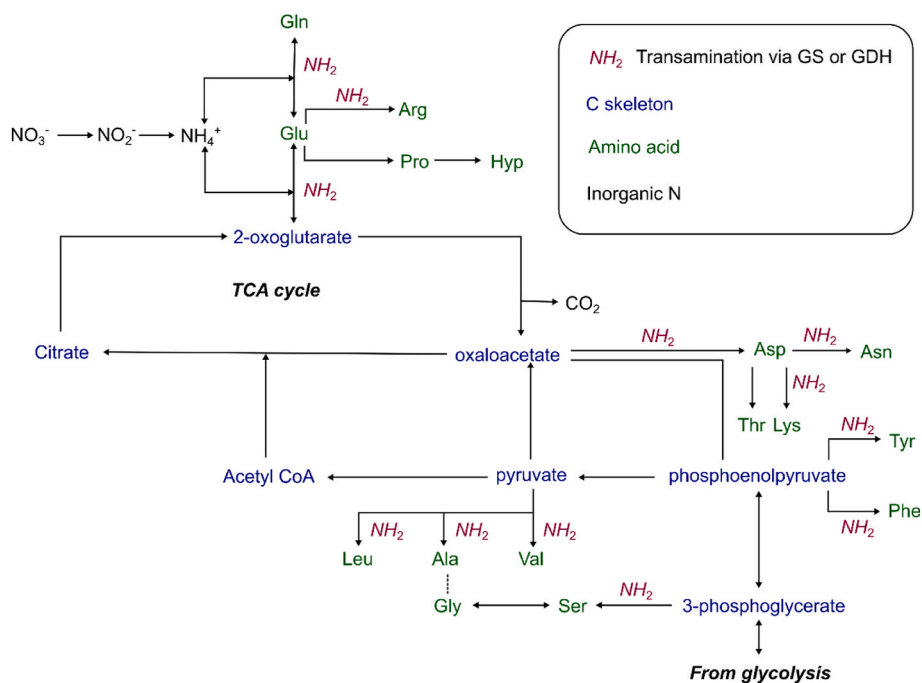
Fig. 6. Biosynthetic pathways for amino acid biosynthesis of nitrate (NO_3^-) and ammonium (NH_4^+). Transamination steps (indicated by NH_2) are mediated by the glutamine synthetase (GS) or glutamate dehydrogenase (GDH) pathways.

there is no direct transamination step in the biosynthesis of Pro.

As with Pro, the major pathway of Ser biosynthesis directly involves a transamination step, where 3-phosphohydroxypyruvate is converted to 3-phosphoserine by 3-phophoserine amino transferase, which is subsequently hydrolysed to Ser (Fig. 6) (Stauffer, 2004). However, Knowles et al. (2010) confirmed, using compound-specific SIP following $^{13}C,^{15}N$-Gly addition, that Ser is also rapidly biosynthesized from Gly, with addition of a hydroxymethyl group by glycine hydroxymethyl-transferase, during the first stage of Gly metabolism (Bourguignon et al., 1988; Schirch and Szebenyi, 2005; Stauffer, 2004). This process is extremely rapid (Knowles et al., 2010) and a contribution of this biosynthesis pathway of Ser from one of the most abundant AA in soil, where transamination is not directly involved may be responsible for the lower observed preference for NH_4^+. Gly could also be considered to be further in biosynthetic proximity to N assimilation given the biosynthetic pathway of Ser (Fig. 6) but had a clear preference for NH_4^+ over NO_3^-, particularly at 55% and 85% WFPS. There is an alternative pathway for Gly biosynthesis, with transfer of NH_2 from Ala to glyoxylate (Caspi et al., 2020; Conley et al., 2017). This has previously been observed as the dominant pathway for Gly biosynthesis in freshwater POM (Mena-Rivera et al., 2022). The results presented in this study suggest that Ala-mediated transamination plays a key role in Gly biosynthesis in this context.

The combined ^{15}N incorporation into THAAs from the separate ^{15}N labelled treatments can be used to assess the overall effects of WFPS on THAA biosynthesis. This assumption was supported by THAA-N concentrations, as a proxy for protein-N, in the separate ^{15}N labelled treatments, which showed the same trends in individual, and total AA concentrations. Moreover, inorganic N concentrations were also consistent between ^{15}N labelled treatments (Loick et al., 2021), thus transformation of $^{15}NH_4^+ = ^{14}NH_4^+$ and $^{15}NO_3^- = ^{14}NO_3^-$. For all WFPS, there was an initial increase in THAA concentration, likely due to the addition of fertiliser-N, however this was short lived (*ca.* 1 d). This short-term change in protein-N concentration due to fertiliser addition has previously been observed for grasslands (Charteris et al., 2016; Reay et al., 2023). The subsequent divergence in THAA concentrations due to WFPS was significant, with increased concentrations at 55% WFPS, and later 85% WFPS, while 70% WFPS did not vary from $t = 0$ concentrations. Increases in concentration suggest more biosynthesis than metabolism of AAs in soil (as FAAs and BAAs) and drying (55% WFPS) and wetting (85% WFPS) the soil induced a shift in the ratio of these processes. Microbial community abundances may also shift with changing WFPS, due to differing moisture optimums (Borowik and Wyszkowska, 2016). The increased THAA concentration at 55% WFPS may have reflected that the microbial community was best suited to this moisture level, as this was closest to the WFPS at the point of sampling in the field (58%), although the soil was air dried (to 35% WFPS) prior to the experiment. Hence, drying and wetting the soils may have induced changes in the homeostasis of the microbial community, and the changes in turnover were reflected in the THAA-N concentration. This is also supported by changes in the relative contribution of nitrifiers and denitrifiers to N_2O fluxes in the same soil (Loick et al., 2021) as well as other grasslands (Bracken et al., 2021). Varying rates of assimilation of fertiliser N within the microbial pool has been elucidated by compound-specific ^{15}N-SIP with amino sugars, a smaller (5–12% of N_{org}), but more specific N_{org} pool (He et al., 2011a; He et al., 2011b; Reay et al., 2019). Slower assimilation of fertiliser-N by fungal communities, and possible shifts in the microbial community structure at differing WFPS may have yielded this observation.

Overall, incorporation of fertiliser-N was significantly affected by WFPS (85% > 55% > 70%). It was hypothesised that there would be higher ^{15}N incorporation at higher WFPS, due to nutrient mobilisation (Misra and Tyler, 1999). While this was the case for the WFPS of 85%, 55% WFPS showed greater incorporation than 70% WFPS. This sequence of treatments was consistent with the observed preference for NH_4^+, and CO_2 fluxes from the same unfertilised grassland (Loick et al.,

2021). It is suggested that the higher microbial activity, indicated by both AA incorporation and respiration at 85% WFPS was due to increased nutrient mobilisation. The 55% WFPS treatment showed little decline in extractable NH_4^+, indicating N availability, and gross N transformations associated with both NH_4^+ and NO_3^- declined at higher WFPS, determined via the *Ntrace* tool (Loick et al., 2021; Müller et al., 2007, 2014). Furthermore, N_2O fluxes were also in the range 85% ≫ 55% > 70%, with the relative contribution of nitrification, heterotrophic nitrification and denitrification varying with WFPS (Bateman and Baggs, 2005; Butterbach-Bahl et al., 2013; Zhang et al., 2015). As suggested from changes in THAA concentrations, there may be shifts in microbial community structure, or activity, due to differing soil moisture optimums (Borowik and Wyszkowska, 2016). Increases in soil respiration are expected with higher soil moisture (Orchard and Cook, 1983), thus deviation from this suggests nutrient availability at 70% may have limited microbial activity, and THAA biosynthesis. Another hypothesis may be that the optimum for both nitrification and denitrification in this soil is *ca.* 70% WFPS, given previous observations of variations with soil texture (Weier et al., 1993), and well-documented evidence for simultaneous nitrification-denitrification in unsaturated soils (Castellano-Hinojosa et al., 2020). Thus, increases in simultaneous microbial activity at this optimum could result in anaerobicity which subsequently restricted N uptake at 70% WFPS, and may also explain the lack of preference for NH_4^+ at this WFPS, with nitrification an alternative fate for this substrate (Linn and Doran, 1984).

The partitioning of soil retained ^{15}N between inorganic pools and organic N was dominated by retention in NH_4^+ and NO_3^-. This was expected given application of NH_4NO_3, yet there was an impact of WFPS. This approach removes variability in retention of ^{15}N in soil *vs.* losses, which were dominated by N_2O in this study, to investigate assimilation of soil available N into the THAA pool. This also revealed changes in ^{15}N present in inorganic N pools. Retention of ^{15}N in extractable NH_4^+ was lower than 50% at the first time point, likely due to adsorption, and subsequent decreases in the NH_4^+ were matched by increases in the NO_3^- pool, consistent with changes in their respective concentrations (Loick et al., 2021). Further, rapid assimilation of NH_4^+ into THAAs over NO_3^- was observed, and this pathway also likely contributed to decreases in the $^{15}NH_4^+$. While there were differing patterns, and rates, of assimilation between WFPS treatments, assimilation after 10 d into the THAA pool did not differ. It is likely that THAA incorporation was a function of soil available N; hence differences after 10 d were not observed when normalised by this. Stabilisation of inorganic N amendments into the largest N_{org} pool, microbial protein, is central to mitigating N losses, and supporting plant N supply. The pattern of incorporation revealed by compound-specific ^{15}N-SIP herein revealed controls of WFPS on the N_{org} pool. Feedbacks of WFPS on microbial N assimilation and N losses (e.g., via denitrification and nitrification, volatilisation and leaching losses) should be investigated in future studies to further elucidate mechanistic controls on these processes.

5. Conclusions & implications

Application of differentially labelled NH_4NO_3 provided mechanistic insights into N preference during its assimilation into the soil microbial protein pool. There was a strong preference for NH_4^+ over NO_3^- for assimilation into the THAA pool, however, preference varied with WFPS. This preference was conserved for AAs in close biosynthetic proximity to a transamination step, but not for those further away from the assimilation of N to C skeletons. The combined treatments revealed differing assimilation pathways into the soil microbial protein pool with WFPS. This was controlled by soil N availability and N losses and reflected microbial activity, as inferred from CO_2 fluxes. These results, for the first time, directly show controls of soil moisture on assimilation of N into the microbial protein pool and highlight the complex interplay between N losses and available N for microbial biosynthesis.

Declaration of competing interest

Data availability

Data will be made available on request.

Acknowledgements and funding

Appendix A. Supplementary data

Supplementary data to this article can be found online at https://doi.org/10.1016/j.soilbio.2023.109114.

References

Adams, E., Frank, L., 2003. Metabolism of Proline and the Hydroxyprolines. https://doi.org/10.1146/ANNUREV.BI.49.070180.005041, 10.1146/Annurev.Bi.49.070180.005041, 49, 1005–1061.

Banerjee, S., Helgason, B., Wang, L., Winsley, T., Ferrari, B.C., Siciliano, S.D., 2016. Legacy effects of soil moisture on microbial community structure and N2O emissions. Soil Biology and Biochemistry 95, 40–50. https://doi.org/10.1016/j.soilbio.2015.12.004.

Barrat, H.A., Evans, J., Chadwick, D.R., Clark, I.M., le Cocq, K., Cardenas, L., 2021. The impact of drought and rewetting on N2O emissions from soil in temperate and Mediterranean climates. European Journal of Soil Science 72 (6), 2504–2516. https://doi.org/10.1111/ejss.13015.

Bateman, E.J., Baggs, E.M., 2005. Contributions of nitrification and denitrification to N2O emissions from soils at different water-filled pore space. Biology and Fertility of Soils 41 (6), 379–388. https://doi.org/10.1007/s00374-005-0858-3.

Berg, A., Sheffield, J., 2018. Climate change and drought: the soil moisture perspective. Current Climate Change Reports 4 (2), 180–191. https://doi.org/10.1007/S40641-018-0095-0/FIGURES/1.

Borowik, A., Wyszkowska, J., 2016. Soil moisture as a factor affecting the microbiological and biochemical activity of soil. Plant Soil and Environment 62 (6), 250–255. https://doi.org/10.17221/158/2016-PSE.

Bourguignon, J., Neuburger, M., Douce, R., 1988. Resolution and characterization of the glycine-cleavage reaction in pea leaf mitochondria. Properties of the forward reaction catalysed by glycine decarboxylase and serine hydroxymethyltransferase. Biochemical Journal 255 (1), 169–178. https://doi.org/10.1042/BJ2550169.

Bracken, C.J., Lanigan, G.J., Richards, K.G., Müller, C., Tracy, S.R., Grant, J., Krol, D.J., Sheridan, H., Lynch, M.B., Grace, C., Fritch, R., Murphy, P.N.C., 2021. Source partitioning using N2O isotopomers and soil WFPS to establish dominant N2O production pathways from different pasture sward compositions. Sci. Total Environ. 781, 146515 https://doi.org/10.1016/J.SCITOTENV.2021.146515.

Butterbach-Bahl, K., Baggs, E.M., Dannenmann, M., Kiese, R., Zechmeister-Boltenstern, S., 2013. Nitrous oxide emissions from soils: how well do we understand the processes and their controls? Philosophical Transactions of the Royal Society B: Biological Sciences 368 (1621). https://doi.org/10.1098/RSTB.2013.0122.

Cárdenas, L.M., Hawkins, J.M.B., Chadwick, D., Scholefield, D., 2003. Biogenic gas emissions from soils measured using a new automated laboratory incubation system. Soil Biology and Biochemistry 35, 867–870. https://doi.org/10.1016/S0038-0717(03)00092-0.

Castellano-Hinojosa, A., Charteris, A.F., Müller, C., Jansen-Willems, A., González-López, J., Bedmar, E.J., Carrillo, P., Cárdenas, L.M., 2020. Occurrence and 15N-quantification of simultaneous nitrification and denitrification in N-fertilised soils incubated under oxygen-limiting conditions. Soil Biol. Biochem. 143, 107757 https://doi.org/10.1016/j.soilbio.2020.107757.

Caspi, R., Billington, R., Keseler, I.M., Kothari, A., Krummenacker, M., Midford, P.E., Ong, W.K., Paley, S., Subhraveti, P., Karp, P.D., 2020. The MetaCyc database of metabolic pathways and enzymes - a 2019 update. Nucleic Acids Research 48 (D1), D445–D453. https://doi.org/10.1093/NAR/GKZ862.

Charteris, A.F., Knowles, T.D.J., Michaelides, K., Evershed, R.P., 2016. Compound specific amino acid 15N stable isotope probing of nitrogen assimilation by the soil microbial biomass using gas chromatography/combustion/isotope ratio mass spectrometry. Rapid Communications in Mass Spectrometry 30 (16), 1846–1856. https://doi.org/10.1002/RCM.7612.

Chiewattanakul, M., McAleer, A.D.A., Reay, M.K., Griffiths, R.I., Buss, H.L., Evershed, R.P., 2022. Compound-specific amino acid 15N-stable isotope probing for the quantification of biological nitrogen fixation in soils. Soil Biology and Biochemistry 169, 108654. https://doi.org/10.1016/j.soilbio.2022.108654.

Christie, P., Wasson, E.A., 2001. Short-term immobilization of ammonium and nitrate added to a grassland soil. Soil Biology and Biochemistry 33 (9), 1277–1278. https://doi.org/10.1016/S0038-0717(00)00237-6.

Clayden, B., Hollis, J.M., 1984. Criteria for Differentiating Soil Series, Soil Survey Technical Monograph, vol. 17. Harpenden, UK.

Conley, M., Mojica, M., Mohammed, F., Chen, K., Napoline, J.W., Pollet, P., Wang, J., Krishnamurthy, R., Liotta, C.L., 2017. Reaction of glycine with glyoxylate: competing transaminations, aldol reactions, and decarboxylations. Journal of Physical Organic Chemistry 30 (12), e3709. https://doi.org/10.1002/poc.3709.

Corr, L.T., Berstan, R., Evershed, R.P., 2007. Optimisation of derivatisation procedures for the determination of δ13C values of amino acids by gas chromatography/combustion/isotope ratio mass spectrometry. Rapid Communications in Mass Spectrometry 21 (23), 3759–3771. https://doi.org/10.1002/rcm.3252.

Csonka, L.N., Leisinger, T., 2007. Biosynthesis of proline. EcoSal Plus 2 (2). https://doi.org/10.1128/ecosalplus.3.6.1.4.

Davidson, E.A., 1993. Soil water content and the ratio of nitrous oxide to nitric oxide emitted from soil. In: Biogeochemistry of Global Change. Springer US, pp. 369–386. https://doi.org/10.1007/978-1-4615-2812-8_20.

Dong, X., Quinn, P.J., Wang, X., 2012. Microbial metabolic engineering for L-threonine production. Subcellular Biochemistry 64, 283–302. https://doi.org/10.1007/978-94-007-5055-5_14/COVER.

Friedel, J.K., Scheller, E., 2002. Composition of hydrolysable amino acids in soil organic matter and soil microbial biomass. Soil Biology and Biochemistry 34 (3), 315–325. https://doi.org/10.1016/S0038-0717(01)00185-7.

Geisseler, D., Horwath, W.R., 2014. Investigating amino acid utilization by soil microorganisms using compound specific stable isotope analysis. Soil Biology and Biochemistry 74, 100–105. https://doi.org/10.1016/J.SOILBIO.2014.02.024.

Geisseler, D., Horwath, W.R., Joergensen, R.G., Ludwig, B., 2010. Pathways of nitrogen utilization by soil microorganisms – a review. Soil Biology and Biochemistry 42 (12), 2058–2067. https://doi.org/10.1016/j.soilbio.2010.08.021.

Giacometti, C., Demyan, M.S., Cavani, L., Marzadori, C., Ciavatta, C., Kandeler, E., 2013. Chemical and microbiological soil quality indicators and their potential to differentiate fertilization regimes in temperate agroecosystems. Applied Soil Ecology 64, 32–48. https://doi.org/10.1016/j.apsoil.2012.10.002.

Harrison-Kirk, T., Beare, M.H., Meenken, E.D., Condron, L.M., 2013. Soil organic matter and texture affect responses to dry/wet cycles: effects on carbon dioxide and nitrous oxide emissions. Soil Biology and Biochemistry 57, 43–55. https://doi.org/10.1016/J.SOILBIO.2012.10.008.

He, H., Li, X.B., Zhang, W., Zhang, X., 2011a. Differentiating the dynamics of native and newly immobilized amino sugars in soil frequently amended with inorganic nitrogen and glucose. European Journal of Soil Science 62 (1), 144–151. https://doi.org/10.1111/j.1365-2389.2010.01324.x.

He, H., Zhang, W., Zhang, X., Xie, H., Zhuang, J., 2011b. Temporal responses of soil microorganisms to substrate addition as indicated by amino sugar differentiation. Soil Biology and Biochemistry 43 (6), 1155–1161. https://doi.org/10.1016/j.soilbio.2011.02.002.

Herron, P.M., Stark, J.M., Holt, C., Hooker, T., Cardon, Z.G., 2009. Microbial growth efficiencies across a soil moisture gradient assessed using 13C-acetic acid vapor and 15N-ammonia gas. Soil Biology and Biochemistry 41 (6), 1262–1269. https://doi.org/10.1016/J.SOILBIO.2009.03.010.

Jones, D.L., Kielland, K., 2012. Amino acid, peptide and protein mineralization dynamics in a taiga forest soil. Soil Biology and Biochemistry 55, 60–69. https://doi.org/10.1016/j.soilbio.2012.06.005.

Kanehisa, M., Furumichi, M., Sato, Y., Kawashima, M., Ishiguro-Watanabe, M., 2022. KEGG for taxonomy-based analysis of pathways and genomes. Nucleic Acids Research. https://doi.org/10.1093/NAR/GKAC963.

Knowles, T.D.J., Chadwick, D.R., Bol, R., Evershed, R.P., 2010. Tracing the rate and extent of N and C flow from 13C,15N-glycine and glutamate into individual de novo synthesised soil amino acids. Organic Geochemistry 41 (12), 1259–1268. https://doi.org/10.1016/j.orggeochem.2010.09.003.

Linn, D.M., Doran, J.W., 1984. Effect of water-filled pore space on carbon dioxide and nitrous oxide production in tilled and nontilled soils. Soil Science Society of America Journal 48 (6), 1267–1272. https://doi.org/10.2136/SSSAJ1984.03615995004800060013X.

Liu, Q., Qiao, N., Xu, X., Xin, X., Han, J.Y., Tian, Y., Ouyang, H., Kuzyakov, Y., 2016. Nitrogen acquisition by plants and microorganisms in a temperate grassland. Scientific Reports 6 (1), 1–10. https://doi.org/10.1038/srep22642, 2016 6:1.

Loick, N., Dixon, E., Matthews, G.P., Müller, C., Ciganda, V.S., López-Aizpún, M., Repullo, M.A., Cardenas, L.M., 2021. Application of a triple 15N tracing technique to elucidate N transformations in a UK grassland soil. Geoderma 385, 114844. https://doi.org/10.1016/J.GEODERMA.2020.114844.

Luo, J., Tillman, R.W., Ball, P.R., 1999. Factors regulating denitrification in a soil under pasture. Soil Biology and Biochemistry 31 (6), 913–927. https://doi.org/10.1016/S0038-0717(99)00013-9.

Ma, Q., Zheng, J., Watanabe, T., Funakawa, S., 2020. Microbial immobilization of ammonium and nitrate fertilizers induced by starch and cellulose in an agricultural

soil, 10.1080/00380768.2020.1843072, 67(1), 89–96. https://doi.org/10.1080/00380768.2020.1843072.

Mena-Rivera, L., Lloyd, C.E.M., Reay, M.K., Goodall, T., Read, D.S., Johnes, P.J., Evershed, R.P., 2022. Tracing carbon and nitrogen microbial assimilation in suspended particles in freshwaters. Biogeochemistry. https://doi.org/10.1007/S10533-022-00915-X.

Misra, A., Tyler, G., 1999. Influence of soil moisture on soil solution chemistry and concentrations of minerals in the calcicoles phleum phleoides and veronica spicata grown on a limestone soil. Annals of Botany 84 (3), 401–410. https://doi.org/10.1006/ANBO.1999.0941.

Müller, C., Laughlin, R.J., Spott, O., Rütting, T., 2014. Quantification of N2O emission pathways via a 15N tracing model. Soil Biology and Biochemistry 72, 44–54. https://doi.org/10.1016/j.soilbio.2014.01.013.

Müller, C., Rütting, T., Kattge, J., Laughlin, R.J.J., Stevens, R.J.J., 2007. Estimation of parameters in complex ^{15}N tracing models by Monte Carlo sampling. Soil Biology and Biochemistry 39 (3), 715–726. https://doi.org/10.1016/j.soilbio.2006.09.021.

Orchard, V.A., Cook, F.J., 1983. Relationship between soil respiration and soil moisture. Soil Biology and Biochemistry 15 (4), 447–453. https://doi.org/10.1016/0038-0717(83)90010-X.

Reay, M.K., Charteris, A.F., Jones, D.L.D.L., Evershed, R.P., 2019. ^{15}N-amino sugar stable isotope probing (^{15}N-SIP) to trace the assimilation of fertiliser-N by soil bacterial and fungal communities. Soil Biology and Biochemistry 138, 107599. https://doi.org/10.1016/j.soilbio.2019.107599.

Reay, M.K., Marsden, K.A., Powell, S., Chadwick, D.R., Jones, D.L., Evershed, R.P., 2023. Combining field and laboratory approaches to quantify N assimilation in a soil microbe-plant-animal grazing land system. Agriculture, Ecosystems & Environment 346, 108338. https://doi.org/10.1016/j.agee.2022.108338.

Reay, M.K., Pears, K.A., Kuhl, A., Evershed, R.P., Murray, P.J., Cardenas, L.M., Dungait, J.A.J., Bull, I.D., Reay, M.K., Pears, K.A., Kuhl, A., Evershed, R.P., Bull, I.D., Murray, P.J., Cardenas, L.M., Dungait, J.A.J., 2022. Mechanisms of nitrogen transfer in a model clover-ryegrass pasture: a ^{15}N-tracer approach. Plant and Soil 1–21. https://doi.org/10.1007/S11104-022-05585-0, 2022.

Recous, S., Mary, B., Faurie, G., 1990. Microbial immobilization of ammonium and nitrate in cultivated soils. Soil Biology and Biochemistry 22 (7), 913–922. https://doi.org/10.1016/0038-0717(90)90129-N.

Reitzer, L., 2004. Biosynthesis of glutamate, aspartate, asparagine, L -alanine, and D -alanine. EcoSal Plus 1 (1). https://doi.org/10.1128/ECOSALPLUS.3.6.1.3/ASSET/A6EF5AE4-4A4C-48F5-B1D0-1E8C24364311/ASSETS/GRAPHIC/3.6.1.3_IG_006 (GIF).

Reitzer, L., 2014. Amino acid synthesis. *Reference Module in biomedical sciences.* https://doi.org/10.1016/B978-0-12-801238-3.02427-2.

Rice, C.W., Tiedje, J.M., 1989. Regulation of nitrate assimilation by ammonium in soils and in isolated soil microorganisms. Soil Biology and Biochemistry 21 (4), 597–602. https://doi.org/10.1016/0038-0717(89)90135-1.

Roberts, P., Jones, D.L., 2008. Critical evaluation of methods for determining total protein in soil solution. Soil Biology and Biochemistry 40 (6), 1485–1495. https://doi.org/10.1016/j.soilbio.2008.01.001.

Saggar, S., Jha, N., Deslippe, J., Bolan, N.S., Luo, J., Giltrap, D.L., Kim, D.-G., Zaman, M., Tillman, R.W., 2013. Denitrification and N2O:N2 production in temperate grasslands: processes, measurements, modelling and mitigating negative impacts. The Science of the Total Environment 465, 173–195. https://doi.org/10.1016/j.scitotenv.2012.11.050.

Schirch, V., Szebenyi, D.M., 2005. Serine hydroxymethyltransferase revisited. Current Opinion in Chemical Biology 9 (5), 482–487. https://doi.org/10.1016/j.cbpa.2005.08.017.

Schulten, H.-R., Schnitzer, M., 1998. The chemistry of soil organic nitrogen: a review. Biology and Fertility of Soils 26 (1), 1–15. https://doi.org/10.1007/s003740050335.

Six, J., Frey, S.D., Thiet, R.K., Batten, K.M., 2006. Bacterial and fungal contributions to carbon sequestration in agroecosystems. Soil Science Society of America Journal 70 (2), 555–569. https://doi.org/10.2136/sssaj2004.0347.

Stauffer, G.v., 2004. Regulation of serine, Glycine, and one-carbon biosynthesis. EcoSal Plus 1 (1). https://doi.org/10.1128/ECOSALPLUS.3.6.1.2/ASSET/B58379FC-A019-4AA0-8F10-25494ACCA442/ASSETS/GRAPHIC/3.6.1.2_FIG_007 (GIF).

Thomsen, I.K., Schjønning, P., Jensen, B., Kristensen, K., Christensen, B.T., 1999. Turnover of organic matter in differently textured soils: II. Microbial activity as influenced by soil water content. Geoderma 89 (3–4), 199–218. https://doi.org/10.1016/S0016-7061(98)00084-6.

Wanek, W., Mooshammer, M., Blöchl, A., Hanreich, A., Richter, A., 2010. Determination of gross rates of amino acid production and immobilization in decomposing leaf litter by a novel ^{15}N isotope pool dilution technique. Soil Biology and Biochemistry 42 (8), 1293–1302. https://doi.org/10.1016/j.soilbio.2010.04.001.

Wardle, D.A., 1998. Controls of temporal variability of the soil microbial biomass: a global-scale synthesis. Soil Biology and Biochemistry 30 (13), 1627–1637. https://doi.org/10.1016/S0038-0717(97)00201-0.

Weier, K.L., Doran, J.W., Power, J.F., Walters, D.T., 1993. Denitrification and the dinitrogen/nitrous oxide ratio as affected by soil water, available carbon, and nitrate. Soil Science Society of America Journal 57 (1), 66–72. https://doi.org/10.2136/SSSAJ1993.03615995005700010013X.

Xue, R., Shen, Y., Marschner, P., 2017. Soil water content during and after plant growth influence nutrient availability and microbial biomass. Journal of Soil Science and Plant Nutrition 17 (3), 702–715. https://doi.org/10.4067/S0718-95162017000300012.

Zhang, J., Müller, C., Cai, Z., 2015. Heterotrophic nitrification of organic N and its contribution to nitrous oxide emissions in soils. Soil Biology and Biochemistry 84, 199–209. https://doi.org/10.1016/j.soilbio.2015.02.028.